Varas, D.; Artero-Guerrero, J. A.; Pernas-Sánchez, J.; López-Puente, J. (2013). "Analysis of high velocity impacts of steel cylinders on thin carbon/epoxy woven laminates". *Composite Structures*, v. 95, January, pp. 623-629.
DOI: 10.1016/j.compstruct.2012.08.015

Proyecto:

DPI2010-15123
CCG10-UC3M/DPI-4694

Analysis of high velocity impacts of steel cylinders on thin carbon/epoxy woven laminates

D. Varas, J.A. Artero-Guerrero, J. Pernas-Sánchez,

J. López-Puente *

Department of Continuum Mechanics and Structural Analysis. University Carlos III of Madrid. Avda. de la Universidad, 30. 28911 Leganés, Madrid, Spain

Key words: Carbon fiber; Composite; Ballistic; Numerical Model; Cohesive elements; Impact.

Abstract

In this work a numerical model was developed to predict the behavior of thin woven laminates under high velocity impacts. The material model, implemented in a user subroutine to be used with a commercial FE code, takes into account different failure mechanisms. The inter-lamina failure prediction is achieved by means of the use of cohesive elements. Finally, in order to validate the model, experimental tests were accomplished in a wide range of velocities from 100 to 400 m/s. Residual velocity of

* Corresponding author. Fax number: 34 916248331. E-mail address: jlpuente@ing.uc3m.es

the projectile and damaged area of the laminates are compared with the numerical results. Once the model is validated, a further investigation has been made in order to analyze the influence of projectile slenderness on the laminate response.

1 Introduction

Aeronautic and aerospace industries play a very important role in the technical development of composite materials. These industries are continuously increasing the use of laminated composite structures, due to their high strength-to-weight and stiffness-to-weight ratios as well as their anisotropic behavior. Those special characteristics allow to optimize designs and fulfil the strict requirements of the mentioned industries. In addition the total mass of the structures is reduced and hence the fuel consumption diminished. Laminated carbon fiber in an epoxy matrix is the most used composite material in structural applications in these sectors because their good combination between mechanical properties, high resistance to corrosion and fatigue, and low density. The reduction of raw material costs, the development of automation of manufacturing processes and the growing experience in design technology have increased the CFRP applications in commercial aircraft, where the percentage of this kind of materials in last designs of aeronautical structures constitute more than the 50% (in terms of weight). Due to the use of these materials in primary structures, it is necessary to understand how composites behave during their service life when they are subjected to the different loads.

Vulnerability studies of CFRP aerospace structures are of great importance in the design of any aircraft. These structures may suffer high velocity loads due to bird strikes or hailstones, especially dangerous because of their high possibility of oc-

currence and their disastrous consequences. Moreover, a stone, small fragment or metallic piece located in the take off runaway, as well as any other kind of debris could impact a fuel tank causing hydrodynamic ram effects and the catastrophic failure of the aircraft [1–7]. The aeroengine turbine blade may also fail due to fatigue and may penetrate the wall of containment cell, damaging oil tanks and airframes [8]. Impact engineering is also of great interest in the field of spacecraft because of the probability of impact between some of the numerous space debris and a satellite or space shuttle structures. CFRPs are well known to be particularly vulnerable to foreign objects impacts, mainly due to the brittleness of the polymeric phase which cause a multiplicity of failure modes and leads to significant strength reduction in post-damage performance. Therefore understanding their response to a range of potential impact loadings and resulting damage mechanisms is essential for the successful use of these materials.

The response of CFRP panels is quite different depending on the velocity of impacts [9]. Numerous works that study the behavior of CFRPs subjected to low velocity impacts have been carried out by means of experimental tests methods such as pendulum impact or drop tower impact. However, the number of papers regarding the behavior of carbon fiber laminates impacted at hundred of meters per second is relatively small. Experimental results of CFRPs impacted by steel projectiles at high velocities can be found in the works of Cantwell and Morton [9], Sun and Potti [10], Larsson [11], Bland and Dear [12], López-Puente et al. [13–15], Will et al. [16], Tanabe et al. [17,18], Hammond et al. [19], Hosur et al. [20], Herzsberg and Weller [21], Caprino et al. [22], and Hazell et al. [23], among others.

The impact process of a projectile onto a composite plate can be described in different phases: initial contact and stress wave propagation, compression and local

punch, plug formation under shear and compression, fiber breakage at the rear layers, and final perforation. During these phases, the initial energy of the projectile is totally or partially absorbed (depends if the projectile is arrested or not) by the laminate and transformed into kinetic energy, strain energy or irrecoverable energy associated to different damage mechanisms, namely matrix cracking, delamination, fiber shear or tensile fiber failure. To predict the behavior of composite laminates, influenced by parameters such as fiber and matrix types, stacking sequence [16], woven or tape architecture [13], stitching [11,20], service temperature [13], impact velocity and angle [9,15] and shape of impactor [24], quite complex numerical [25] or analytical [9,22,26,27] simulation models have been developed by different authors.

This work proposes a numerical methodology to predict the response of carbon/epoxy woven laminates under high velocity impacts. A material model which takes into account different intra-laminar failure mechanisms, such as fiber failure in both fiber directions and in plane and out of plane matrix failure, was implemented through a user subroutine; in addition the use of cohesive elements allow to reproduce the inter-lamina failure. The finite element code ABAQUS/Explicit was used in the numerical simulations. In order to validate the numerical simulations, experimental tests were performed. A lightweight gas gun was used to carry out impacts of a steel cylindrical projectile onto carbon epoxy woven laminates at different velocities. The residual velocity of the projectile, in case of perforation, and the damaged area of the laminates were measured to validate the numerical results. In addition once the numerical model is validated, a further investigation has been made in order to analyze the influence of projectile slenderness on the laminate response.

2 Experimental tests

In order to have experimental data to validate the numerical model that will be proposed, impact tests were performed. Carbon/epoxy laminated plates with 10 plies, $([0])_{10}$), a total thickness of 2.0 mm and a size of 80×80 mm^2 were impacted with a steel projectile. Afterwards the mentioned specimens were inspected by means of a non-destructive technique to measure the damaged area.

2.1 Impact tests

The projectile consisted on a tempered steel cylinder with a diameter of 5.5 mm and a mass of 1.1 g. The tempered steel is hard enough to ensure that no plastic deformation occurs during penetration, simplifying the analysis because all the energy associated to the projectile is kinetic. The wide range of impact velocities performed ($100 - 400\ m/s$) allows to obtain the minimum velocity at which the projectile perforates the laminate plate, known as ballistic limit.

The set-up employed in the impact tests consists on a one-stage light gas gun which uses helium at a pressure of up to 200 bar to impel the projectile up to 500 m/s against the plate. The projectile travels through a gallery in which two photoelectric cells detect the passing of the projectile, obtaining the impact velocity. At the end of the gallery, the projectile reaches an armored chamber ($1 \times 1 \times 1\ m^3$), inside of which the specimen is placed. The appropriate position of the plate is ensured by means of a support that avoids the movement of the edges of the specimen. The windows included on the armor chamber, one in a lateral side and another on the top, allow to light inside the chamber and to capture the video sequence of the

impact. Fig. 1 shows a sketch of the experimental device used for impact tests.

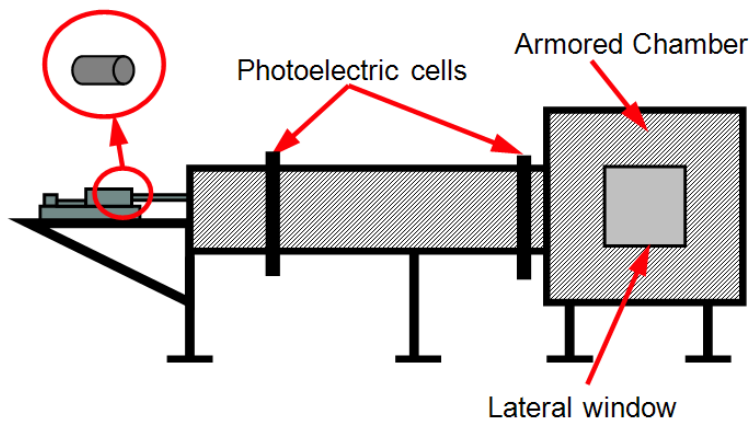

Fig. 1. Sketch of the experimental device.

A Photron Ultima APX digital high-speed camera was employed to measure the residual velocity when the projectile perforates the plate. The selected frame rate (15000 frames per second), resolution (1024 x 128 pixels) and the shutter time ($11\mu s$) were chosen based on early testing and represent an optimal trade off between available lighting and the minimization of blur in the images. The camera was placed on the top of the chamber allowing the perfect capture of the entry the exit of the projectile trough the laminate. A sequence recorded by the high speed camera is shown in Fig. 2. It is easy to determine the residual velocity using an image treatment software, because the Δt between the two instants is pre-configured in the camera, and the distance traveled by the projectile is scaled using the length of the projectile or even the millimeter paper.

2.2 Damage inspection tests

Once the specimen is impacted, it is analyzed in order to know the extension of the damage. To achieve this, the specimens are inspected using the C-scan ultrasonic

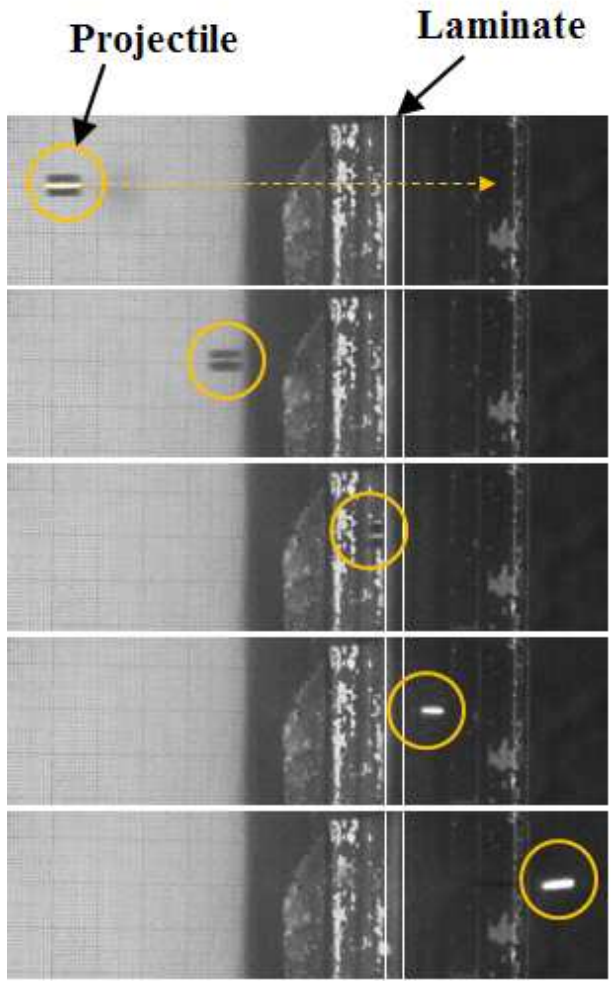

Fig. 2. Sequence of impact process.

method, Fig. 3. The ultrasonic techniques are based on the elastic waves attenuation passing through discontinuities of a continuum media, as delaminations or another kind of damage. A computer processes the ultrasonic waves and shows a two-dimensional image of the waves attenuation which represents the damage extension of each specimen. Fig. 4 shows an example of the inspection.

Fig. 3. Non-destructive inspection device.

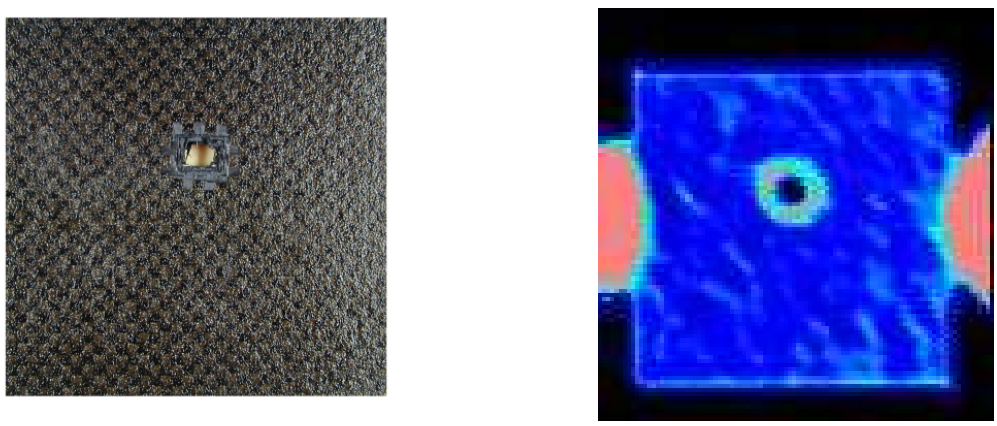

Fig. 4. Left: Impacted specimen. Right: Non-destructive inspection of the specimen.

3 Numerical simulations

The numerical model has been developed in the commercial finite element code Abaqus/Explicit v6.10. This code allows describing the material behavior through a user subroutine written in Fortran; this option has been used in this work to model the response of the carbon/epoxy woven laminate.

3.1 Material modeling

To reproduce the process of impact of a projectile onto a plate, it is necessary to define the material models of both solids. The projectile used in the experiments was made of steel, and by the fact that no plastic deformation was observed after penetration during the test campaign, a linear elastic behavior was chosen for the simulations, with the following values: $E = 210\ GPa$, $\nu = 0.3$ and $\rho = 7850\ kg/m^3$.

The carbon/epoxy woven laminate has been modeled as an orthotropic elastic material until failure. This kind of approach has been widely used in impact problems on composite materials; some examples are the model of Hou et al. [28] for tape laminates or the model of J. López-Puente et al. [15] for woven laminates. To model how the material fails, different damage mechanisms are defined, both intra-laminar and inter-laminar. The inter-laminar failure has been implemented by means of a user subroutine (VUMAT) whereas the inter-laminar failure has been taken into account using cohesive elements. Following, the different failure modes are described.

3.1.1 Intra-laminar failure criteria

- Fibre failure

  This failure mechanism is related to the failure of carbon fibers. Woven laminates have fibers in orthogonal in-plane directions (1 and 2); hence two different equations are considered in order to take into account both fill and warp directions.

The equations that describe the failure are:

$$d_{f1} = \begin{cases} \dfrac{\sigma_{11}}{X_t} \;\; if \;\; \sigma_{11} > 0 \\ \\ \dfrac{|\sigma_{11}|}{X_c} \;\; if \;\; \sigma_{11} < 0 \end{cases} \tag{1}$$

$$d_{f2} = \begin{cases} \dfrac{\sigma_{22}}{Y_t} \;\; if \;\; \sigma_{22} > 0 \\ \\ \dfrac{|\sigma_{22}|}{Y_c} \;\; if \;\; \sigma_{22} < 0 \end{cases} \tag{2}$$

where σ_{11} and σ_{22} are the stresses in the warp and fill direction respectively, X_t and X_c are the strengths of the composite laminate in tension and compression for the warp direction, and finally Y_t and Y_c are the strengths in tension and compression for the fill direction.

- Crushing matrix failure.

  Two different parameters are proposed in this damage mechanism, one in plane direction (d_{m12}), an the other one in the through-thickness direction (d_{m3}). The corresponding equations are:

$$d_{m12} = \frac{\sigma_{12}}{S_{12}} \tag{3}$$

$$d_{m3} = \frac{1}{4}\left(\frac{\sigma_{33}}{Z_c}\right)^2 + \frac{Z_c \cdot \sigma_{33}}{4S_{13}S_{23}} + \left|\frac{\sigma_{33}}{Z_c}\right| + max\left[\left(\frac{\sigma_{13}}{S_{13}}\right)^2, \left(\frac{\sigma_{23}}{S_{23}}\right)^2\right] \tag{4}$$

  where σ_{ij} are components of the stress tensor, S_{12}, S_{13} and S_{23} are the shear strengths in the three different planes and finally Z_c is the strength in the through-thickness direction under compression. The equation 4 applies only when $\sigma_{33} < 0$.

When one of the damage parameters described reaches the value of 1, the stress components involved in the failure definition (fibre or matrix failure) are set to zero (i.e. for $d_{f1} = 0$, then $\sigma_{11} = 0$). Fig. 5 shows the stress tensor components that are

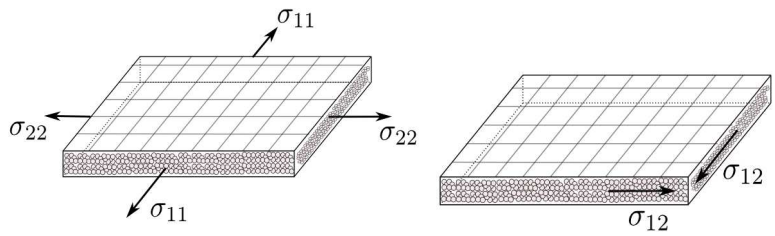

(a) Fiber failure (b) Shear matrix failure

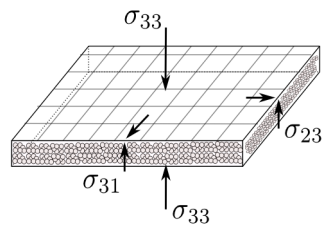

(c) Crushing matrix failure

Fig. 5. Stress tensor componentes in each failure mode

taken into account for each failure mode.

The element erosion is controlled by the total strain; after each time increment the strain tensor is calculated, if one of the components reaches a critical value, then the element is removed. The material constants for the carbon fibre woven laminates used in the simulations are presented in table 1. All the values were provided by the composite manufacturer.

3.1.2 Inter-laminar failure criteria

- Delamination

  To model the delamination that appears between two layers it is necessary to define, as in any failure mechanism, a damage initiation criterion and a damage evolution law. Some authors such as Lee [29] and Hashin [30] define the beginning

$E_1 = E_2$	E_3	ν_{12}	$\nu_{13} = \nu_{23}$	G_{12}	$G_{23} = G_{13}$
68 GPa	10 GPa	0.22	0.49	5 GPa	4.5 GPa
$X_t = Y_t = X_c = Y_c$	Z_c	Z_r	$\varepsilon_1 = \varepsilon_2$	ε_3	$\varepsilon_{12} = \varepsilon_{23} = \varepsilon_{13}$
880 MPa	340 MPa	96 MPa	0.025	0.05	0.1

Table 1

Properties of woven carbon/epoxy laminate.

of the delamination by means of a criteria based on normal and shear stresses:

$$\left(\frac{\sigma_{33}}{t_n}\right)^2 + \left(\frac{\sigma_{13}}{t_s}\right)^2 + \left(\frac{\sigma_{23}}{t_t}\right)^2 \geq 1 \tag{5}$$

where t_n, t_s and t_t are the strengths of the cohesive interface in the normal and in the two shear directions respectively. This last equation is applied if one of the following conditions is reached:

$$\sigma_{33} \geq Z_t \quad or \quad \sqrt{\sigma_{12}^2 + \sigma_{13}^2} \geq S_{23} \tag{6}$$

where Z_t is the laminate strength under tension in the through thickness direction. Different laws for the damage evolution can be found. Some of the most used are defined based on the energy that is dissipated as a result of the damage process, also called fracture energy. Some examples of these laws are the proposed by Benzeggagh- Kenane [31] or the potential laws [32], which are expressed in the following equations respectively:

$$G_n^C + (G_s^C - G_n^C)\{\frac{G_S}{G_T}\}^\eta = G^C \tag{7}$$

$$\left(\frac{G_n}{G_n^C}\right)^\alpha + \left(\frac{G_s}{G_s^C}\right)^\alpha + \left(\frac{G_t}{G_t^C}\right)^\alpha = 1 \tag{8}$$

where G_n, G_s and G_t are the released rates energies in the three aforementioned directions, G_n^C, G_s^C and G_t^C are the critical values of the released rates energies,

and finally α and η are parameters of the models. This initiation and evolution damage models have been implemented in finite element codes such as ABAQUS by means of the so called cohesive elements. Some examples of the use of cohesive elements to model the delamination can be found in the works of Camanho et al. [33], Turon et al. [34], Elmarakbi et al. [35], Lopes [36] or Khokhar [37].

The cohesive elements are based on a constitutive response in terms of a traction-separation law. Fig. 6 schematically depicts this law for a failure mode type I. To define the law it is necessary to specify the linear elastic behavior by means of the correspondent stiffness (K_{nn}, K_{ss} and K_{tt}), the initiation of the damage by means of the interface resistance (t_n, t_s and t_t) and the damage evolution by means of the critical released rate energies (G_n^C, G_s^C and G_t^C).

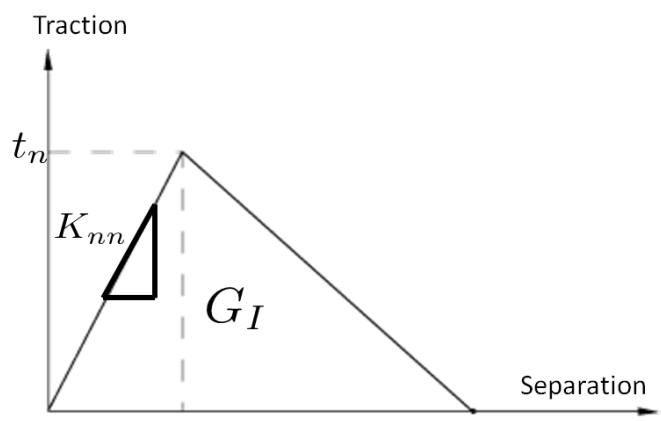

Fig. 6. Typical traction-separation response in a cohesive material [32]

In this work, a quadratic nominal stress criterion for the damage initiation, similar to equation 5, has been chosen. The damage evolution law is a potential law type based on energies as the equation 8 in which $\alpha = 1$. The properties that have been used are shown in Table 2.

K_{nn}	$K_{ss} = K_{tt}$	t_n	$t_s = t_t$	G_I	$G_{II} = G_{III}$
2 GPa/mm	1.5 GPa/mm	11 MPa	45 MPa	0.6 J/m^2	1.8 J/m^2

Table 2

Parameters for the cohesive interface.

3.2 Finite element mesh

Both the laminate and the projectile were discretized by means of hexahedral elements. In order to obtain reliable results and, based on previous numerical tests, 10 elements were used along the laminate thickness, one per layer. As said, the delamination is modeled by means of cohesive elements. In this numerical model, only one layer of cohesive elements, in the middle of the laminate, have been used. This has been considered as an appropriate way of reproducing the delamination damage as well as to reduce the computational cost that would result using a cohesive element layer between each ply of the laminate; the amount of energy absorbed by this damage mechanism is very low compared to the others that participate in the impact process [26]. Finally, the model has 57546 hexahedral elements and 6400 cohesive elements. Boundary conditions were set to the laminate bottom exterior edge, to fulfill the experimental set-up; in this zone the displacement in the projectile velocity direction was impeded.

4 Validation

To validate the numerical model proposed, the residual velocity of the projectile and the damaged area obtained from the experimental tests were compared with the numerical data from the simulations. Fig. 8 shows the residual velocity versus the impact velocity for both experimental and numerical results; it is clear that the

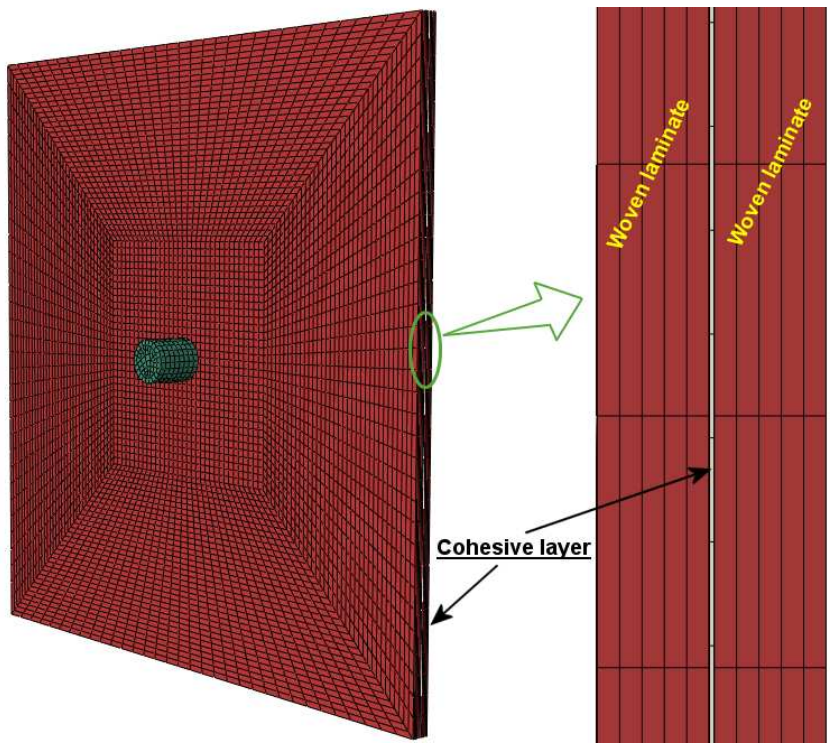

Fig. 7. Mesh of the model and detail of the cohesive layer (right).

model reproduces faithfully the energy loss on carbon/epoxy woven laminates. In addition it has been found that for this type of projectile and laminate the ballistic limit is around 140 m/s.

Fig. 9 depicts the comparison between the delaminated area measured after the impact tests and the numerical data obtained from the simulations. Although differences in the values are appreciated, both the experimental and numerical data show the same trends. Before the ballistic limit, the delaminated area grows rapidly since all the projectile energy is absorbed mainly as damage. Once the "critical" velocity is reached, the delaminated area decreases tending to an asymptotic value that coincides with the front area of the projectile. Similar results were found in previous works [15].

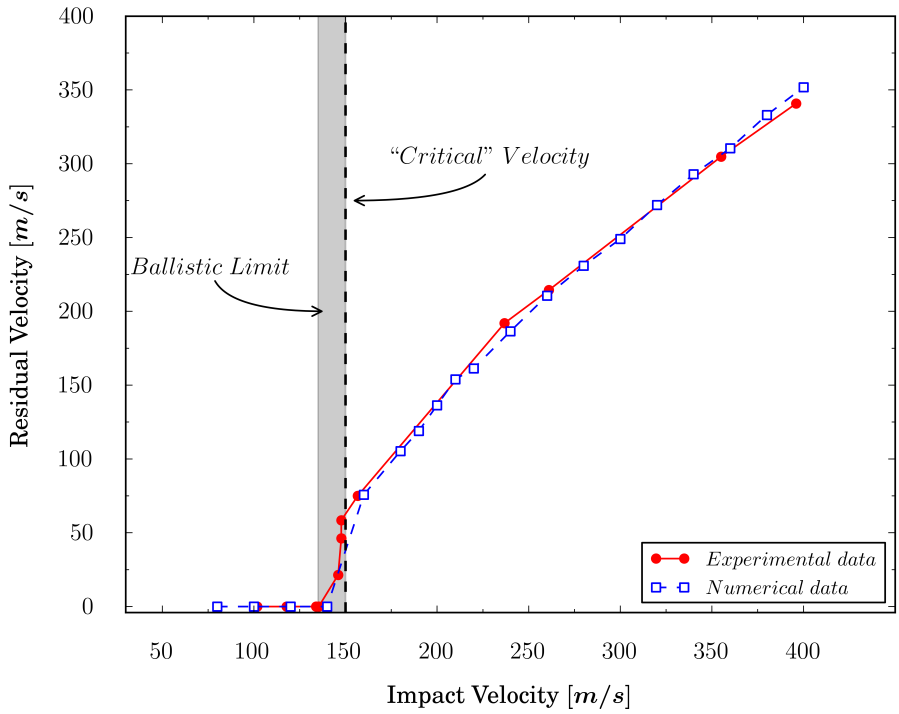

Fig. 8. Residual velocity vs. impact velocity. Experimental and numerical results.

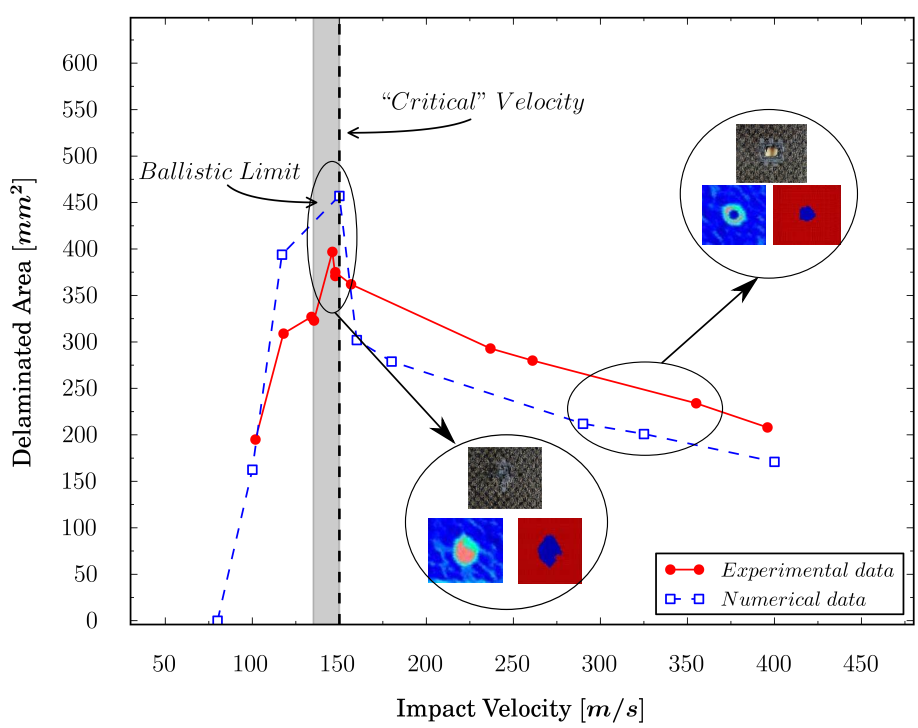

Fig. 9. Delaminated area vs. impact velocity. Experimental and numerical results.

5 Analysis of the influence of projectile aspect ratio in residual velocity

Once the numerical model is validated with the experimental test it is possible to analyze the influence of the projectile slenderness in the residual velocity keeping the mass constant. Three different cylindrical impactors where numerically studied (Table 3).

	height [mm]	radius [mm]	Aspect ratio
Type A	4	3.36	0.59
Type B	6	2.75	1.09
Type C	10	2.13	2.16

Table 3

Studied projectiles.

The residual velocity vs. the impact velocity for the aforementioned projectile geometries is depicted in Fig 10. Although the kinetic energy of all the projectiles considered are the same, the behavior of the laminates is completely different. It can be observed that the ballistic limit for the different geometries varies; when the projectile has a smaller impact area (projectile Type C) the ballistic limit is lower than a projectile that posses the same kinetic energy with a bigger impact area (projectile Type A). At high velocities the three curves tend to a straight line with similar slopes.

The relation between the projectile radius and the residual velocity can be explained taking into account that the kinetic energy of the projectile is absorbed mainly by

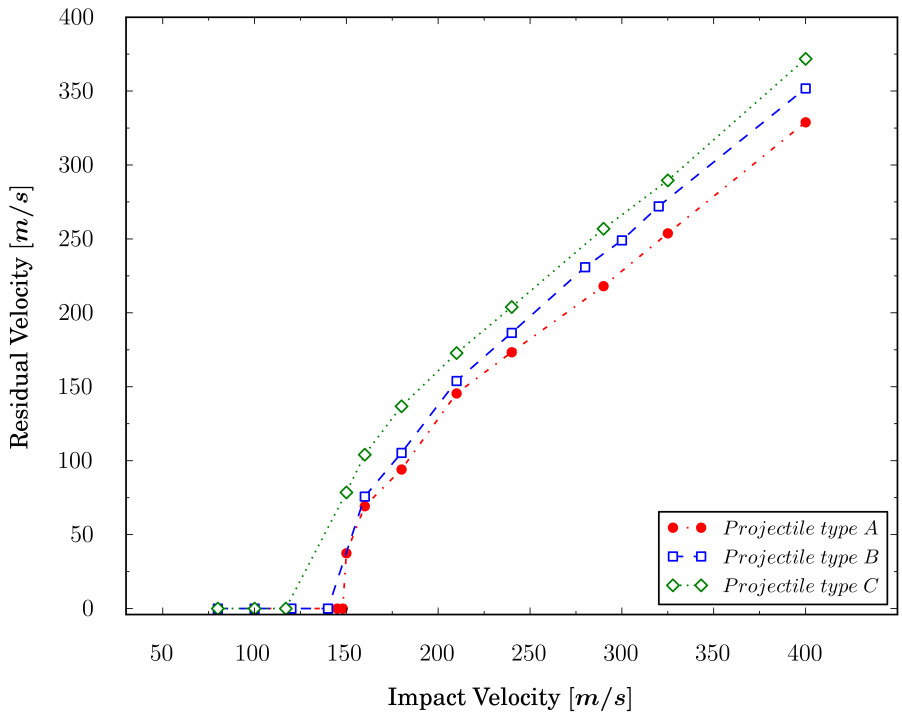

Fig. 10. Residual velocity vs. impact velocity for the different projectiles studied.

two different mechanisms; linear momentum transferred from the projectile to the detached part of laminate and laminate breakage due to crushing. This assumption is valid for velocities above the ballistic limit [26,27].

The energy absorbed by linear momentum transfer is due to the fact that the laminate volume that is in front of the projectile impact area is accelerated from the rest to the current projectile velocity, and it is assumed to remain attached to the projectile during the penetration. The associated amount of energy is written as:

$$E_m = \frac{1}{2}\left(\pi R^2 h \rho_l\right) V_r^2 \tag{9}$$

where R is the radius of the projectile, h is the thickness of the laminate, ρ_l is the density of the laminate (the term in brackets represent the accelerated mass of the laminate) and V_r is the residual velocity.

The energy absorbed by laminate crushing is related to the breakage of the laminate by compression because of the projectile impact. The energy associated to this mechanism is evaluated as the product of the trough-thickness compressive strength of the laminate σ_c, the projectile frontal area πR^2 and the distance that the projectile travels in the laminate h. This term is written as follows:

$$E_c = \sigma_c \pi R^2 h \tag{10}$$

Finally, the energy balance can be expressed as:

$$\frac{1}{2} m_p \left(V_i^2 - V_r^2 \right) = E_m + E_c \tag{11}$$

where m_p is the mass of the projectile (constant for all the studied cases) and V_i the impact velocity. Rearranging the terms it is possible to rewrite the expression to show how the radius affects the residual velocity:

$$V_r^2 = \frac{m_p V_i^2 - 2\pi R^2 h \sigma_c}{m_p + \pi R^2 h \rho_l} \tag{12}$$

The equation 12 shows that if the radius of the projectile is increased and all other parameters remain constant (as in the cases in study), the residual velocity decreases. These are the trends observed in Fig. 10 where the values of the residual velocity that correspond to the projectile with the smallest radius (Type C) are bigger than the rest of the cases.

6 Conclusions

In this work, a numerical model to predict the response of carbon/epoxy woven laminates under high velocity impacts has been developed. The numerical simula-

tions predict faithfully the residual velocity of the projectile; this capacity is of great importance in order to study the behavior of aeronautic structures under such kind of impacts, reducing considerably the number of experimental test. In addition, the damaged area trends are well reproduced by the model. After validating the model by means of experimental test, a study of the influence of the projectile aspect ratio, keeping constant the projectile mass, has been carried out. A clear influence of the projectile radius in the residual velocity has been observed and explained.

Acknowledgements

This research was done with the financial support of the Spanish Ministry of Education under Project reference DPI2010-15123 and of the Region of Madrid and University Carlos III of Madrid under Project reference CCG10-UC3M/DPI-4694.

References

[1] Airoldi A, Cacchione B, Modelling of impact forces and pressures in Lagrangian bird strike analyses, Int. J. Impact Eng 32 (2006) 1651–1677.

[2] Anghileri M, Castelletti LML, Invernizzi F, Mascheroni M, A survey of numerical models for hail impact analysis using explicit finite element codes, International Journal of Impact Engineering 31 (2005) 929–944.

[3] Mines RAW, McKown S, Birch RS, Impact of aircraft rubber tyre fragments on aluminium alloy plates: I-experimental, International Journal of Impact Engineering 34 (2007) 627–646.

[4] Varas D, López-Puente J, Zaera R, Experimental analysis of fluid-filled aluminium tubes subjected to high-velocity impact, International Journal of

Impact Engineering 36 (2009) 81–91.

[5] Varas D, Zaera R, López-Puente J, Numerical modelling of the hydrodynamic ram phenomenon, International Journal of Impact Engineering 36 (2009) 363–374.

[6] Varas D, López-Puente J, Zaera R, Numerical modelling of partially filled aircraft fuel tanks submitted to Hydrodynamic Ram, Aerospace Science and Technology 16 (2011) 19–28.

[7] Varas D, Zaera R, López-Puente J, Experimental study of CFRP fluid-filled tubes subjected to high-velocity impact, Composite Structures 93 (2011) 2598–2609.

[8] Hai-jun X, Rong-ren W, Aeroengine turbine blade containment tests using hig-speed rotor spin test facility, Aerospace Science and Technology 10 (2006) 501–508.

[9] Cantwell WJ, Morton J, Comparison of low and high velocity impact response of CFRP, Composites 20(6) (1989) 545–551.

[10] Sun CT, Potti V, A simple model to predict residual velocities of thick composite laminates subjected to high velocity impact, International Journal of Impact Engineering 18(3) (1996) 339–353.

[11] Larsson F, Damage tolerance of a stitched carbon/epoxy laminate, Composites Part A: applied science and manufacturing 28 923–934.

[12] Bland PW, Dear JP, Observations on the impact behaviour of carbon-fibre reinforced polymers for the qualitative validation of models, Composites Part A: applied science and manufacturing 32 (2001) 1217–1227.

[13] López-Puente J, Zaera R, Navarro C, The effect of low temperatures on the intermediate and high velocity impact response of CFRP, Composites: Part B 33 (2002) 559–566.

[14] López-Puente J, Zaera R, Navarro C, High energy impact on woven laminates, Journal de Physique IV 110 (2003) 639–644.

[15] López-Puente J, Zaera R, Navarro C, Experimental and numerical analysis of normal and oblique ballistic impacts on thin carbon/epoxy woven laminates, Composites: Part A 39 (2008) 374–387.

[16] Will MA, Franz T, Nurick GN, The effect of laminate stacking sequence of CFRP filament wound tubes subjected to projectile impact, Composites Structures 58 (2002) 259–270.

[17] Tanabe Y, Aoki M, Fujii K, Kasano H, Yasuda E, Fracture behavior of cfrps impacted by relatively high-velocity steel sphere, International Journal of Impact Engineering 28 (2003) 627–642.

[18] Tanabe Y, Aoki M, Stress and strain measurements in carbon-related materials impacted by a high-velocity steel sphere, International Journal of Impact Engineering 28 (2003) 1045–1059.

[19] Hammond RI, Proud WG, Goldrein HT, Field JE, High-resolution optical study of the impact of carbon-fibre reinforcedpolymers with different lay-ups, International Journal of Impact Engineering 30 (2004) 69–86.

[20] Hosur MV, Vaidya UK, Ulven C, Jeelani S, Performance of stitched/unstitched woven carbon/epoxy composites under high velocity impact loading, Composite Structures 64 (2004) 455–466.

[21] Herzsberg I, Weller T, Impact damage resistance of buckled carbon/epoxy panels, Composite Structures 73 (2006) 130–137.

[22] Caprino G, Lopresto V, Santoro D, Ballistic impact behaviour of stitched graphite/epoxy laminates, Composites Science and Technology 67 (2007) 325–335.

[23] Hazell PJ, Kister G, Stennett C, Bourque P, Cooper G, Normal and oblique penetration of woven CFRP laminates by a high velocity steel sphere, Composites: Part A 39 (2008) 866–874.

[24] Mines RAW, Roach AM, Jones N, High velocity perforation behaviour of polymer composite laminates, International Journal of Impact Engineering 22 (1999) 561–588.

[25] Fernández-Fdz D, López-Puente J, Zaera R, Prediction of the behaviour of CFRPs against high-velocity impact of solids employing an artificial neural network methodology, Composites: Part A 39 (2008) 989–996.

[26] López-Puente J, Zaera R, Navarro C, An analytical model for high velocity impacts on thin cfrps woven laminates, International Journal of Solids and Structures 44 (2007) 2837-2851.

[27] López-Puente J, Varas D, Loya JA, Zaera R, Analytical modelling of high velocity impacts of cylindrical projectiles on carbon/epoxy laminates, Composites: Part A 40 (2009) 1223–1230.

[28] Hou JP, Petrinic N, Ruiz C, Hallett SR, Prediction of impact damage in composite plates, Composites Science and Technology 60:2, (2000) 273-281.

[29] Fish JC, Lee SW, Delamination of tapered composite structures, Engineering Fracture Mechanics 34:1 (1989) 43-54.

[30] Hashin Z, Failure criteria for unidirectional fiber composites, Transactions of the ASME. Journal of Applied Mechanics 47:2 (1980) 329-34.

[31] Benzeggagh ML and Kenane M, Measurement of Mixed-Mode Delamination Fracture Toughness of Unidirectional Glass/Epoxy Composites with Mixed-Mode Bending Apparatus, Composites Science and Technology 56 (1996) 439-449.

[32] Abaqus Explicit Manual, version 6.10 Edition,HKS 2010

[33] Camanho PP, and Davila CG, Mixed-Mode Decohesion Finite Elements for the Simulation of Delamination in Composite Materials, NASA/TM-2002-211737, 1-37, 2002.

[34] Turon A, Camanho PP, Costa J, Dávila CJ, A damage model for the simulation of delamination in advanced composites under variablemode loading, Mechanics of Materials 38:11 (2006) 1072-1089.

[35] Elmarakbi AM, Hu N, Fukunaga H, Finite element simulation of delamination growth in composite materials using LS-DYNA, Composite Science and Technology 69 (2009), 2383-2391

[36] Lopes CS, Camanho PP, Gürdal Z, Maimí P, González EV, Low-velocity impact damage on dispersed stacking sequence laminates.Part II: Numerical simulations, Composites Science and technology 69 (2009) 937-947

[37] Khokhar ZR, Ashcroft IA, Silberschmidt VV, Simulations of delamination in CFRP laminates: Effect of microstructural randomness, Computational material science 46 (2009) 607-613